Ge/SiGe Quantum Well Waveguide Modulator Monolithically Integrated With SOI Waveguides

Shen Ren, Yiwen Rong, Stephanie A. Claussen, Rebecca K. Schaevitz, Theodore I. Kamins, *Fellow, IEEE*, James S. Harris, *Fellow, IEEE*, and David A. B. Miller, *Fellow, IEEE*

***Abstract*— We report a Ge/SiGe quantum well waveguide electroabsorption modulator that is monolithically integrated with silicon-on-insulator waveguides. The active quantum well section is selectively grown on a silicon-on-insulator substrate and has a footprint of 8 μm^2. The integrated device demonstrates more than 3.2-dB contrast ratio with 1-V direct voltage swing at 3.5 GHz. We also show the potential of this device to operate in the telecommunication C-band at room temperature.**

***Index Terms*— Germanium quantum well, optical interconnects, optical waveguide modulator, optoelectronics, quantum-confined Stark effect.**

I. Introduction

OPTICAL interconnects are a promising solution to the interconnect bottleneck for current information processing technology [1,2]. A complementary metal-oxide-semiconductor (CMOS) compatible, energy efficient optical modulator is a key building block for optical interconnect systems. Modulators using refractive index changes in Si are attractive but are either relatively large with correspondingly large operating energies (see, e.g., Refs. [3,4]) or must exploit high-Q resonators (e.g., Ref [5]) or slow light structures [6] to magnify the field amplitude. High-Q resonators in particular require precise tuning and temperature stabilization, which itself can dissipate significant power.

Electroabsorption modulators, by contrast, may be relatively small even without resonators, and may require little or no temperature tuning. Silicon-germanium (SiGe) Franz-Keldysh electroabsorption modulators have been demonstrated recently using bulk germanium (Ge) on silicon (Si) [7,8]. In 2005, we demonstrated quantum-confined Stark effect (QCSE) electroabsorption in Ge quantum well (QW) structures on Si substrates [9,10]. By changing the applied electrical field across the QWs, the absorption coefficient of the structure can be significantly modified. The relative strength of this electroabsorption opens a new approach to realizing efficient, CMOS-compatible optical modulation. Several stand-alone optical modulators and photodetectors based on Ge/SiGe QWs have already been successfully demonstrated [11,12]. In this letter, we report the first Ge/SiGe QCSE QW waveguide modulator that is monolithically integrated with the silicon-on-insulator (SOI) waveguides through direct-butt coupling and selective epitaxial growth. The active section of the device has a footprint of only 8 μm^2, and can provide an optical modulation of 3.2 dB with a 1 V swing. Modulation measurements show that the integrated device should be able to operate at 7.0 Gbps and beyond.

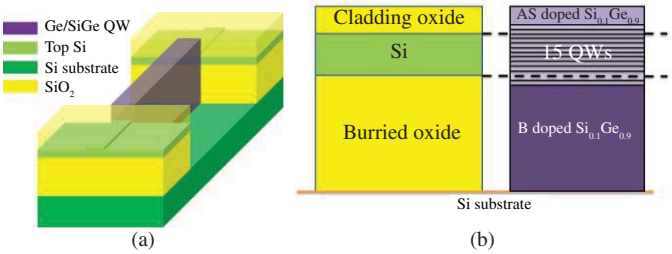

Fig. 1. Schematic of the integrated device. (a) Perspective view of the Ge/SiGe QW modulator with SOI ridge waveguides. (b) Cross-sectional view of the SOI waveguide section and the modulator active section.

II. Device Design and Fabrication

The schematic of the integrated quantum well modulator is shown in Fig. (1a). 800 nm wide SOI ridge waveguides act as the bus waveguides for routing the optical signals on chip. The top Si layer is 310 nm thick, on top of a 1 μm thick buried oxide (BOX). We designed the waveguide to be single-moded, supporting only the fundamental quasi transverse electric (TE) mode.

The active modulator section consists of a vertical p-i-n diode with 15 pairs of Ge/$Si_{0.15}Ge_{0.85}$ QWs in the intrinsic region. The thicknesses of wells and barriers are 12 nm and 20 nm, respectively. To accommodate the relaxed SiGe buffer, the BOX layer of the SOI is removed in the active section. The optical coupling between the SOI waveguide and the active section is realized through direct butt-coupling. The epitaxy is

Manuscript received August 28, 2011; revised December 6, 2011; accepted December 20, 2011. Date of publication December 23, 2011; date of current version February 23, 2012. This work was supported in part by DARPA MTO Office under the UNIC Program under Contract Agreement with Oracle HR0011-08-09-0001 and in part by the SRC/DARPA FCRP IFC. This work was performed in part by the Stanford Nanofabrication Facility.

S. Ren was with the Department of Electrical Engineering, Stanford University, Stanford, CA 94536 USA. He is now with the San Jose Research Center, Hitachi Global Storage Technologies, San Jose, CA 95135 USA (e-mail: renshen07@gmail.com).

Y. Rong was with the Department of Electrical Engineering, Stanford University, Stanford, CA 94536 USA. He is now with Philips Lumileds Inc., San Jose, CA 95134 USA (e-mail: rywryw@gmail.com).

S. A. Claussen, R. K. Schaevitz, T. I. Kamins, J. S. Harris, and D. A. B. Miller are with the Department of Electrical Engineering, Stanford University, Stanford, CA 94536 USA (e-mail: sclaussen@stanford.edu; rschaevitz@stanford.edu; kamins@stanford.edu; harris@snow.stanford.edu; dabm@stanford.edu).

Color versions of one or more of the figures in this letter are available online at http://ieeexplore.ieee.org.

Digital Object Identifier 10.1109/LPT.2011.2181496

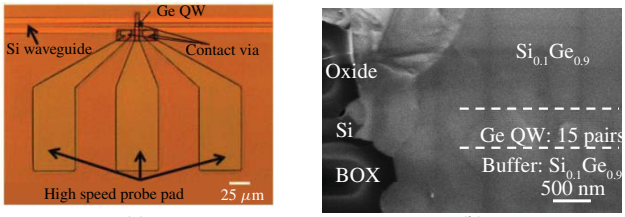

Fig. 2. Images of the fabricated device. (a) Top-view optical microscope image, showing the entrance/exit ridge SOI waveguide and the active Ge/SiGe modulator section. (b) Cross section SEM image of the fabricated device at the boundary of the growth window.

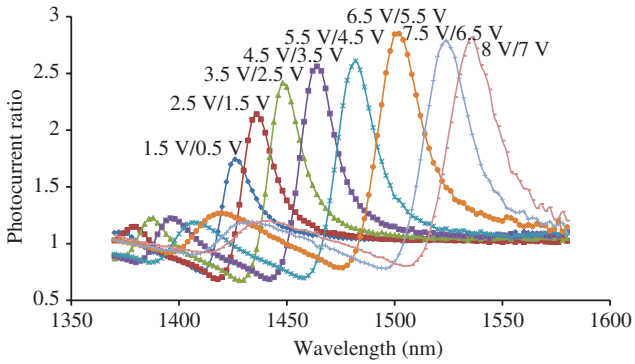

Fig. 3. Photocurrent ratio with a 1-V swing at different bias voltages at room temperature.

designed such that the Si core of the SOI waveguide and the QWs of the active section are on the same vertical level with maximum overlap, as shown in Fig. (1b). This ensures that the optical mode in the SOI waveguide can be efficiently modulated by the Ge QWs when passing through the active section.

First, the ridge waveguide is defined by etching away 60 nm of the top Si layer. Then a 1.5 μm thick SiO_2 layer is deposited, acting as the upper cladding for the SOI waveguide and the growth mask for the subsequent selective epitaxial growth. Growth windows for the active sections are defined and etched all the way to the Si handle substrate. A special 20 nm thick SiO_2 spacer is deposited on the sidewall of the growth window using a dual-layer process to prevent lateral growth from the exposed Si layer. Detailed discussion of the spacer, including its impact on insertion loss and fabrication, can be found in [13]. A selective epitaxial growth step is then carried out to deposit the p-i-n Ge/SiGe QWs inside the growth window. The top and bottom layers of the SiGe epitaxy are *in-situ* doped with arsenic and boron, respectively, making it possible to apply an electric field across the quantum wells. Details of the selective epitaxial process can be found in [14]. After the growth, a chemical mechanical polishing (CMP) step is carried out to planarize the structures. Finally, lithography, reactive ion etching, metal deposition, and liftoff define the active waveguide modulator and make contacts to the doped p- and n- layers of the active section. We note that all the fabrication steps for this device can be done in an advanced CMOS foundry. In particular, all the lithography steps are carried out using ASML I-line photolithography; no electron-beam lithography is needed.

After the fabrication, the chip is diced and facet-polished to an optical finish. Fig. 2(a) shows a top-view optical microscope image of the fabricated device. Fig. 2(b) is a scanning electron microscope (SEM) image showing the cross section at the boundary of the growth window. From the figure, we can see that the Si core of the ridge waveguide and the QWs are, indeed, well aligned vertically.

III. Measurement Results

First, we measured the surface normal modulators on the fabricated chip. Optical output from a tunable laser is incident on the top surface of the device. Photocurrent is collected at various bias voltages at room temperature through a lock-in amplifier. Fig. (3) shows the photocurrent ratio spectra under a 1 V swing for a 150 μm by 150 μm square surface normal modulator at room temperature (the photocurrent spectra can be found in Ref. [14]). The dark current densities at -1V and -8V are 2.2mA/cm^2 and 12mA/cm^2, respectively. The ratio of photocurrent expresses the modulation depth compared to the material background loss. This is an important figure of merit for electroabsorption modulator material. We also show results with only 1V of drive swing, which corresponds to the scale of voltage drive available from simple CMOS driver circuits. The largest photocurrent ratio for a 1V drive swing is 2.84, occurring right at 1500 nm for a voltage swing between 6.5 V and 5.5 V. With a 7.5 V bias and 1V swing, the photocurrent ratio is larger than 2 from 1526 nm to 1548 nm, corresponding to a 3 dB optical bandwidth of 2.8 THz, covering more than half of the telecommunication C-band (1530 nm $\sim$ 1565 nm). This indicates that the QCSE based Ge/SiGe QW modulator can operate in the C-band at room temperature. The large operating bias voltage range available means in practice that the wavelength range of this modulator can be tuned by changing the bias voltage rather than by some other mechanism, such as heating.

Following surface normal calibration of photocurrent, waveguide transmission measurements were carried out. Tapered fibers with a spot size of 2.5 μm were used to couple light into and out of the waveguide chip. From passive waveguide links with varying lengths, we determine that the propagation loss of the SOI ridge waveguide is 0.9 dB/cm. Though the waveguide loss was low, the overall loss from waveguide input to waveguide output in this first demonstration was relatively high (15 dB in the "transmitting" state of the modulators). This loss is due to the mode mismatch between the thin Si waveguide core (310 nm) and the thick Ge/SiGe grown modulator region ($\sim$1.5 μm), which starts at the Si handle wafer surface, as shown in Fig. (1b). This thick Ge/SiGe region leads to a waveguide core of the same vertical thickness, bounded by the top interface and the interface of the grown SiGe and the underlying Si handle wafer. We estimate from FDTD simulations that the total coupling loss from the input to the output Si waveguides due to this height mismatch is $\sim$12 dB. This excess loss could be alleviated in future devices by starting with a selective regrowth of Si to reduce the required thickness of SiGe growth.

The experiment setup for the active link characterization is shown in Fig. (4a). A high speed probe is used to deliver a high

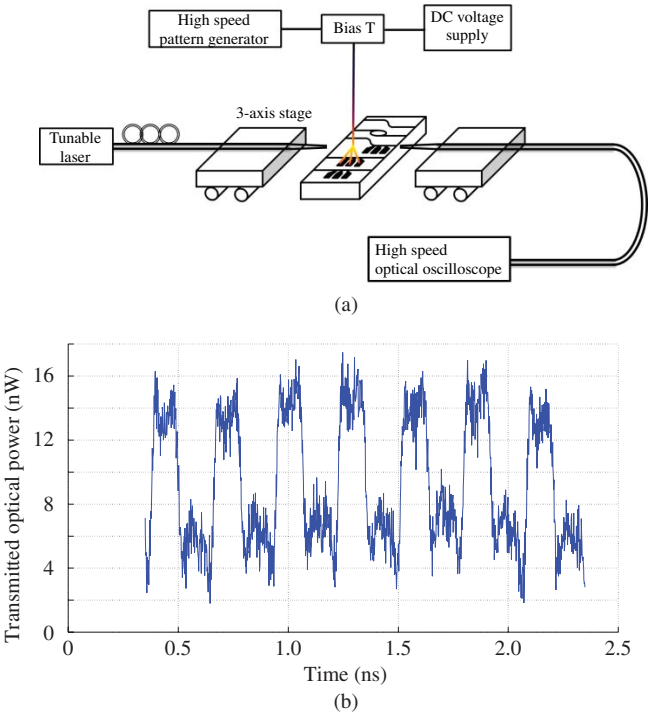

Fig. 4. High-speed measurement results. (a) Setup schematic for the waveguide transmission measurement. (b) Oscilloscope trace of the transmitted optical signal under high-speed electrical signal.

speed electrical signal from a pattern generator (HP 8813A) to the waveguide modulator. The optical output from a tunable laser couples into the entrance passive Si waveguide, passes through the active Ge/SiGe waveguide modulator, where it is modulated, and eventually collected from the exit passive Si waveguide into a high speed optical oscilloscope (Agilent 86100A). The input optical power from the laser source is kept at 500 μW at all wavelengths. Fig. 4(b) shows the measurement results for a waveguide link with an active modulator section 800 nm wide and 10 μm long (with a calculated internal capacitance of $\sim$3 fF). A 4 V D.C. bias and 1V swing are combined by a bias T and applied to the device under test. The laser wavelength is fixed at 1460 nm. Fig. 4(b) shows the oscilloscope signal of the transmitted optical power through the waveguide link under a square wave drive at 3.5 GHz, which would directly indicate at least 7 Gb/s non-return-to-zero modulation capability, with more than 3 dB extinction ratio. Furthermore, the sharp rise and fall times in Fig. 4(b) indicate that the device can operate at even higher frequencies.

IV. Conclusion

In summary, we demonstrated a Ge/SiGe QCSE QW waveguide modulator that is integrated with SOI waveguides through direct-butt coupling and selective epitaxial growth. The active section of the integrated device has a footprint of only 8 μm^2. The waveguide modulator provides direct modulation of more than 3 dB under 1V swing. Further improvements to better mode-match the QW section and the SOI waveguide sections can greatly reduce the insertion loss of the current device. This promises ultra-compact, ultra-low power, CMOS compatible optical modulators for on-chip interconnect applications.

Acknowledgment

The authors would like to acknowledge Dr. P. Dong, Dr. S. Liao, Dr. D. Feng, Dr. H. Liang, Dr. R. Shafiiha, and Dr. M. Asghari from Kotura Inc., Monterey Park, CA, for technical assistance in waveguide fabrication. They also would like to acknowledge the generous technical support from ASML Inc., Veldhoven, The Netherlands.

References

[1] R. Soref, "The past, present and future of silicon photonics," *IEEE. J. Sel. Topics Quantum Electron.*, vol. 12, no. 6, pp. 1678–1687, Nov. 2006.

[2] D. Miller, "Device requirements for optical interconnects to silicon chips," *Proc. IEEE*, vol. 97, no. 7, pp. 1166–1185, Jul. 2009.

[3] A. Liu, *et al.*, "A high-speed silicon optical modulator based on a metal-oxide-semiconductor capacitor," *Nature*, vol. 427, pp. 615–618, Feb. 2004.

[4] Q. Xu, B. Schmidt, S. Pradhan, and M. Lipson, "Micrometer-scale silicon electro-optic modulator," *Nature*, vol. 435, pp. 325–327, May 2005.

[5] L. Gu, W. Jiang, X. Chen, and R. T. Chen, "Physical mechanicsm of p-i-n-diode-based photonic crystal silicon electrooptic modulators for gigahertz operation," *IEEE J. Sel. Topics Quantum Electron.*, vol. 14, no. 4, pp. 1132–1139, Jul./Aug. 2008.

[6] Q. Xu, S. Manipatruni, B. Schmidt, J. Shakya, and M. Lipson, "12.5 Gbit/s carrier-injection-based silicon micro-ring silicon modulators," *Opt. Express*, vol. 15, no. 2, pp. 430–436, 2007.

[7] J. Liu, *et al.*, "Waveguide-integrated, ultralow-energy GeSi electro-absorption modulators," *Nature Photon.*, vol. 2, pp. 433–437, Jul. 2008.

[8] N.-N. Feng, *et al.*, "30 GHz Ge electro-absorption modulator integrated with 3 μm silicon-on-insulator waveguide," *Opt. Express*, vol. 19, no. 8, pp. 7062–7067, 2011.

[9] Y. Kuo, *et al.*, "Strong quantum-confined Stark effect in germanium quantum-well structures on silicon," *Nature*, vol. 437, pp. 1334–1336, Oct. 2005.

[10] Y. Kuo, *et al.*, "Quantum-confined Stark effect in Ge/SiGe quantum wells on Si for optical modulators," *IEEE J. Sel. Top. Quantum Electron.*, vol. 12, no. 6, pp. 1503–1513, Nov. 2006.

[11] J. E. Roth, *et al.*, "C-band side-entry Ge quantum-well electroabsorption modulator on SOI operating at 1 V swing," *Electron. Lett.*, vol. 44, no. 1, pp. 49–50, Jan. 2008.

[12] P. Chaisakul, *et al.*, "Ge/SiGe multiple quantum well photodiode with 30 GHz bandwidth," *Appl. Phys. Lett.*, vol. 98, pp. 131112-1–1131112-3, Mar. 2011.

[13] S. Ren, T. I. Kamins, and D. A. B. Miller, "Thin dielectric spacer for the monolithic integratioun of bulk germanium or germanium quantum wells with silicon-on-insulator waveguides," *IEEE Photon. J.*, vol. 3, no. 4, pp. 739–747, Aug. 2011.

[14] S. Ren, Y. Rong, T. I. Kamins, J. S. Harris, and D. A. B. Miller, "Selective epitaxial growth of Ge/$Si_{0.15}Ge_{0.85}$ quantum wells on Si substrate using reduced pressure chemical vapor deposition," *Appl. Phys. Lett.*, vol. 98, no. 15, pp. 151108-1–151108-3, 2011.